Polymer 51 (2010) 4259–4266

Contents lists available at ScienceDirect

Polymer

journal homepage: www.elsevier.com/locate/polymer

Polymer interphase structure near nanoscale inclusions: Comparison between random walk theory and experiment

Jeffrey S. Meth*, Steven Raymond Lustig

DuPont Nanocomposite Technologies, Central Research & Development, E.I. DuPont de Nemours & Co., Inc., P.O. Box 80400, Wilmington, DE 19880-0400, United States

ARTICLE INFO

Article history:
Received 7 April 2010
Received in revised form
18 June 2010
Accepted 23 June 2010
Available online 30 June 2010

Keywords:
Nanocomposite
Modeling
Random walk

ABSTRACT

We propose a theory for the structure of the interphase in polymeric nanocomposites based on the freely-jointed chain near an impermeable spherical inclusion. The theory considers only the entropic exclusion between a polymer and the inclusion. The radius of gyration of the polymer chain and its distortion from spherical symmetry are perturbed strongly when the chain end is closer than $3R_{g0}$ from the surface of the sphere, where R_{g0} is the unperturbed radius of gyration. Also, the maximum expansion of the chain is bounded by $(4/3)^{1/2}$, equal to a 15% increase. The shape of the polymer chain is elongated tangentially to the surface when the chain end originates in the interphase, but elongates radially due to entropic repulsion when the chain end is very close to the surface of the sphere. All the distortions of the polymer conformation from ideality, and hence the spatial extent of the interphase, occur within the depletion region associated with colloids. The model is used to explain recent experimental results showing that polymer chain dimensions increase in the presence of nanoparticles. The model quantitatively reproduces the observations at low filler loadings using no adjustable parameters, suggesting that entropic arguments can describe the majority of the effect there.

1. Introduction

Polymers in confined geometries such as nanocomposites and thin films are receiving increased attention [1–7]. Nanocomposites are an important class of materials that can display enhanced thermomechanical and barrier properties [7–10]. Thin films show altered glass transition temperatures [4], which has implications for nanoimprint lithography and other electronic applications [11]. Mechanistic explanations for these effects from theoretical and computational modeling are not yet satisfactory as there is a wide range of conflicting predictions and empirical measurements. There is discussion in the field about the interphase, also referred to as the rigid amorphous fraction – a polymeric region surrounding a nanoparticle, that has physical properties different from the bulk polymer [6,7,9,10]. Our hypothesis is that if such an interphase exists, it must have certain structural attributes. If the polymer chains comprising the interphase have the same conformations as the bulk polymer, then no change in properties should be expected, assuming that no chains are tethered to the surface. Only when the polymer conformation deviates from the bulk conformation could one expect a variation in any property. Thus, it is important to understand the structure of the interphase.

Many efforts, both experimental and theoretical, have been undertaken to shed light on the subject of the conformation of a polymer chain in the neighborhood of a nanoparticle or a surface. The presence of an obstacle is expected to perturb the dimensions of a polymer chain. This perturbation may then alter some physical properties of the material, such as radius of gyration, moduli, melt viscosity or strain-at-break. This perturbed region might then be associated with the interphase. A related problem comes from the field of colloids, where it is known that, in the neighborhood of an individual colloid particle, there is a region surrounding the particle that has lower polymer segment density [12–16]. Understanding it is critical for stabilization of colloids. Most work focuses on the extent of the depletion region, but not the conformation of the polymer chains within it.

A wide range of theoretical models and computational simulations have been applied to understanding polymer structure and properties of nanocomposites. Although a complete literature review is outside the scope of this article, to date there is no unifying theme that consistently explains the statistical conformations and orientation of polymer chains in nanocomposites – whether or not any unusual features exist. There is a considerable literature investigating lattice chain-inclusion systems. For example, Ozmusul [17] developed a cubic lattice Monte Carlo simulation wherein self-avoiding polymer beads have fluctuating bond lengths and attractive square well interactions between bead–bead and bead-filler sites. Interestingly,

* Corresponding author. Tel.: +1 302 695 1129.
E-mail address: jeff.meth@usa.dupont.com (J.S. Meth).

0032-3861/$ – see front matter © 2010 Elsevier Ltd. All rights reserved.
doi:10.1016/j.polymer.2010.06.043

the presence of up to 27 vol% small filler particles does not affect the average end-to-end distance statistics relative to simulations without filler particles. From this study we would conclude that nanoparticles do not affect equilibrium melt chain conformations. More recently Termonia [18] has provided a cubic lattice Monte Carlo simulation of self-avoiding polymer beads having constant bond lengths but no other bead–bead or bead-filler interactions. Having considered the presence of up to 20 vol% small filler particles, these simulations indicate the presence of a thin, interfacial region within which polymer segments orient tangentially to the filler particles. This orientation would not be present without the presence of filler particles, so from this study we would conclude that nanoparticles do affect equilibrium melt chain conformations.

There are also seemingly contradictory results from off-lattice simulations. Vacatello [19–22] provides Monte Carlo simulations of realistically-dense linear chains and comparably sized filler particles present up to 36 vol%. The chains comprise beads with fixed separation interacting with immediately neighboring beads by a quadratic bending potential which is minimized when the neighboring segments are perfectly straight. Beads interact with other beads and filler particles with truncated 6-12 Lennard-Jones potentials, which provide substantial attraction between beads and filler particles. Within a few bead shells of the filler particles, beads develop a very thin liquid-like radial distribution function structure with orientation tangential to the filler. Although the characteristic ratio of the mean-square end-to-end distance to the mean-square radius of gyration conforms to unperturbed Gaussian values, the mean squared end-to-end distance in the presence of filler is always smaller than in the unperturbed melt. This is observed even when the filler particles are smaller than the polymer. In contrast Sharaf, Mark and collaborators [23–25] use an off-lattice Monte Carlo methodology for phantom polymer chains described by segments conforming to rotational isomeric state torsion probabilities and are excluded by spherical filler nanoparticles. These simulations show significant departures from unperturbed, Gaussian conformational statistics. Chains are extended relative to unfilled systems when encompassing smaller filler particles, while chains are compressed when ensconsing larger filler particles. Starr and coworkers [26] simulate the molecular dynamics of relatively short, linear FENE bead-spring chains with both attractive and non-attractive truncated Lennard-Jones potentials for bead–bead and bead-filler particles. Here the filler particles are fixed into icosahedral inclusions. The flat surfaces provide a preferential orientation for the polymers, and this effect persists for a distance of roughly one chain radius of gyration. Moreover as chains approach the particle surface the overall radius of gyration increases about 25% while the component perpendicular to the surface decreases more than a factor of 2 for both attractive and non-attractive systems. However the chains retain Gaussian conformational statistics near the nanoparticle surface since the mean-square end-to-end distance is about six times the mean-square radius of gyration, even though the monomer probability distribution function is anisotropic. Most recently, Frischknecht and coworkers applied a self-consistent polymer reference site model to a nanocomposite system and demonstrated increasing chain expansion as a function of particle loading [27]. The polymers are treated as chains of spheres, the particles are spheres, and the total packing fraction is 45%. Site–site interactions are described by Lennard-Jones potentials, where the monomer–monomer and particle–particle interactions are purely repulsive while monomer–particle interactions are purely attractive. The chain expansion is most simply described as due to the attractive interactions between the monomers and the particles; the nanoparticles act as a good solvent. With suitable adjustable scaling, the theory is able to fit the data of Tuteja [28]. However, the approach does not spatially map the orientation and deformation of polymer chains as function of distance of the chain from the surface of the nanoparticle.

Experimentally, measurements of polymer chain dimensions in nanocomposites remains elusive because it is difficult to produce samples with sufficient dispersion quality. Sen's work [29] on colloidal silica loaded polystyrene showed no deviation from Gaussian statistics, but their dispersions were not ideal at high loadings. Jones [30,31] results in thin polystyrene films show that chain dimensions remain Gaussian in the plane of the film. No conclusion could be made about the dimensions perpendicular to the conformations within the confining planes. Nakatani [32,33] showed that chain dimensions in PDMS increased with filler loading, and the magnitude of the effect depended on the molecular weight of the polymer. Recently, Tuteja [28] showed that polystyrene chain dimensions increased in the presence of cross-linked polystyrene-like nanoparticles. We believe their work is the most rigorous to date, but there is currently no theory that can be applied to predict their experimental observables.

With all of this accumulated effort as a backdrop, it is apparent that there is still a need for a generalized theory of the structure of the interphase. Our work intends to add to the body of literature by providing a treatment of a freely-jointed, phantom chain interphase by using the analytic Green's function for a random walk around a sphere. This solution considers entropic exclusion, without energetic interactions between the particle and the polymer. It is the simplest standard treatment for a polymer chain subject to a constraint with this geometry, but has not yet been considered in the literature. The need for this treatment has been identified [25] because the results provide limiting behavior of conformational statistics for finite chains that are prohibitively time consuming to model with computer simulation. Furthermore this model provides limiting behavior to test the more complex Monte Carlo and molecular dynamics simulations whose validity requires highly sophisticated phase space sampling techniques. From this analysis, the radius of gyration, R_g, is calculated, along with the distortion, described by a conformation tensor [34]. We will show that these results compare favorably to the experimental results of Tuteja at low volume concentrations, where it is valid to consider the chain as a random walk around a single sphere, but fail at the highest volume loading [28], where the chain would need to be modeled as a random walk in the presence of several spheres. Polymer segment densities and depletion widths are also calculated, and those results compare well to similar theories from the colloid literature [13].

2. Theory

For a random walk in the vicinity of an impenetrable sphere of radius a, the Green's function satisfies the equation:

$$\left(\frac{\partial}{\partial N} - \frac{l^2}{6}\frac{\partial^2}{\partial \vec{R}^2}\right) G(\vec{R}, \vec{R'}, N, a) = \delta(\vec{R} - \vec{R'})\delta(N) \tag{1}$$

with the boundary condition:

$$G(\vec{R}, \vec{R'}, N, a) = 0 \tag{2}$$

when $\vec{R}$ is on the surface of the sphere. Although the Green's function is symmetric, for bookkeeping purposes we say that the chain begins at $\vec{R}$ and ends at $\vec{R'}$. The polymer chain consists of N steps, each of length l.

This problem is exactly analogous to that of the flow of heat in an infinite region, where the region is bounded internally by the sphere $|\vec{R}| = R = a$. The solution, given by Carslaw and Jaeger [35], is:

$$G(\vec{R},\vec{R}',N,a) = \frac{1}{4\pi\sqrt{RR'}}\sum_{n=0}^{\infty}(2n+1)P_n(\mu)\int_0^{\infty}\frac{C_{n+1/2}(uR)C_{n+1/2}(uR')}{J_{n+1/2}^2(ua)+Y_{n+1/2}^2(ua)}e^{-R_{g0}^2u^2}u\,du \tag{3}$$

$$C_{n+1/2}(z) = J_{n+1/2}(z)Y_{n+1/2}(ua) - Y_{n+1/2}(z)J_{n+1/2}(ua) \tag{3a}$$

In this expression, J is the Bessel's function of the first kind, Y is the Bessel's function of the second kind, P is the Legendre polynomial of argument $\mu=\cos\varphi$, where φ is the angle between the vectors $\vec{R}$ and $\vec{R}'$, and $R_{g0}^2=Nl^2/6$ is the radius of gyration of an unperturbed Gaussian chain. The center of the sphere is the center of the coordinate system.

Using $b=|\vec{R}|-a$ to represent the magnitude of the distance from the chain origin to the surface of the nanoparticle, equation (3) was integrated over all space to arrive at this closed form:

$$G_0(R,N,a) = \int_0^{2\pi}\int_0^{\pi}\int_a^{\infty}G(\vec{R},\vec{R}',N,a)\,R'^2dR'\sin\phi\,d\phi\,d\theta = 1-\frac{a}{b}erfc\left(\frac{b-a}{2R_{g0}}\right) \tag{4}$$

This integral is used to normalize the integrals of the moments, to be calculated below, and was first mentioned by Doi [36]. Using this expression for the normalization integral, we can calculate the total number of configurations in the system:

$$\Omega = \iint G(\vec{R},\vec{R}',N,a)\,d^3\vec{R}\,d^3\vec{R}' \tag{5}$$

So, compared to a Gaussian chain, the chain near the nanoparticle has its number of configurations reduced by (see Appendix B):

$$\Omega_p = \Omega_0-\Omega = \frac{4\pi a^3}{3}\left[1+\frac{6}{\sqrt{\pi}}\frac{R_{g0}}{a}+\frac{3R_{g0}^2}{a^2}\right] \tag{6}$$

Ω_0 is the number of configurations available to the unperturbed Gaussian chain. This is also known as the depleted volume in the literature, and has been previously derived by others by different methods [37–39].

The expression for the mean-squared, end-to-end distance $\langle R_{ee}^2\rangle = \langle(\vec{R}-\vec{R}')^2\rangle$, was evaluated from the integral representation:

$$\left\langle R_{ee}^2(\vec{R},N,a)\right\rangle = \frac{\int\int\int\left(R^2+R'^2-2RR'\cos\phi\right)\,G(\vec{R},\vec{R}',N,a)\,R'^2dR'\,\sin\phi\,d\phi\,d\theta}{\int G(\vec{R},\vec{R}',N,a)\,d^3\vec{R}'} \tag{7}$$

Note that the chain dimensions vary in space relative to the location of the sphere, and its size. The problem is greatly simplified by recognizing a unique property of Legendre polynomials. When integrating G with respect to the polar angle ϕ, only a single Legendre polynomial will integrate to a nonzero value, *e.g.*, in the case of the normalization integral, only the $n=0$ term is not zero after integration. Thus, while it is necessary to evaluate many terms to describe the full shape of the Green's function, only a few terms are needed to evaluate the statistical averages. After equation (7) is split into its three component integrals, we find that the first two integrals can be expressed analytically because of the simple forms for $J_{1/2}$ and $Y_{1/2}$, but the third integral needs to be evaluated numerically.

Using the expression for $\langle R_{ee}^2\rangle$, we calculate the radius of gyration, R_g^2, with the relationship (see Appendix C) [40]:

$$R_g^2(\vec{R},N,a) = \frac{1}{2N^2}\sum_{n=1}^{N}\sum_{m=1}^{N}\left\langle(R_n-R_m)^2\right\rangle \tag{8}$$

The contour plot for the scaled radius of gyration, R_g/R_{g0}, is presented in Fig. 1, where the variables $\alpha=a/2R_{g0}$ and $\beta=b/2R_{g0}$ have been introduced to scale the results. We see that when the particle becomes vanishingly small, $\alpha\to 0$, Gaussian chain statistics are recovered. When the particle becomes very large compared to the size of the polymer, then $\langle R_{ee}^2\rangle$ and R_g match what one would expect from the solution for a random walk near a wall (see Appendix A). For that limiting case, the expression for the mean-squared end-to-end distance (normalized to the unperturbed value) is:

$$\frac{R_{ee,W}^2}{R_{ee,0}^2} = \frac{1}{3}\left(3-4\beta^2\frac{erfc(\beta)}{erf(\beta)}+\frac{2\beta}{\sqrt{\pi}}\frac{e^{-\beta^2}}{erf(\beta)}\right) \tag{9}$$

While other properties derived from this form of the Green's function for the wall match those in the literature (such as segment density, addressed below), this expression for $R_{ee,W}$ has not, to our knowledge, previously appeared in the literature. Between these two limits, we observe the smooth variation of R_g as the radius of the sphere changes. For the large α case, there is a broad, shallow minimum of $R_g/R_{g0}=0.98$ when $\beta=0.9$. It equals one when $\beta=0.50$, and then continues to $R_g/R_{g0}\to(4/3)^{1/2}=1.15$ as $\beta\to 0$. Thus, when the chain origin is very near the surface of the sphere, $\beta<<1$, entropic repulsion causes the chain to expand. As α decreases, we see that the chain becomes less compressed at $\beta=0.9$, and there is less expansion as $\beta\to 0$. The location of the point where R_g is unperturbed stays constant until $\alpha<0.5$, when it begins to move closer to the surface of the sphere.

To calculate the shape of the polymer chain in the presence of the sphere, we calculate the projection of R_{ee} in the radial direction, and in the plane perpendicular to it. This is accomplished using a conformation tensor [34], which we calculate as follows:

$$C_{i,j}(\vec{R},N,a) = \frac{1}{2R_{go}^2}\frac{\int(\vec{R}-\vec{R}')_i(\vec{R}-\vec{R}')_jG(\vec{R},\vec{R}',N,a)d^3\vec{R}'}{\int G(\vec{R},\vec{R}',N,a)d^3\vec{R}'} \tag{10}$$

From this, we define $\Delta=C_{\perp}-C_{\parallel}$ as a proxy for the departure of the statistically averaged chain from spherical symmetry (the perpendicular direction is the radial direction, and the parallel direction is in the plane parallel to the tangent to the surface). For

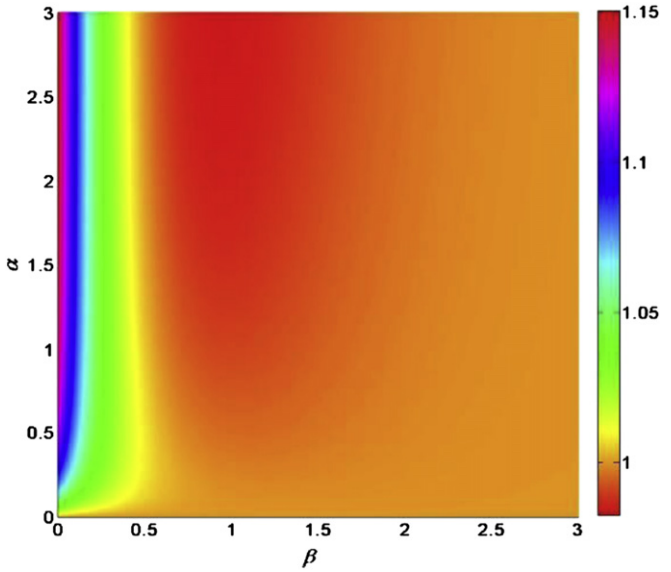

Fig. 1. Normalized radius of gyration for a polymer chain near a sphere. α is the scaled particle radius, and β is the scaled distance from the chain origin to the surface.

$C_\perp$, we use $(\vec{R}-\vec{R'})_i(\vec{R}-\vec{R'})_j = R^2+R'^2-2RR'\cos\phi-R'^2\sin^2\phi$, while for $C_\parallel$, we use $(\vec{R}-\vec{R'})_i(\vec{R}-\vec{R'})_j = R'^2\sin^2\phi$. This accounts for the fact that the end-to-end distance needs to be calculated with the origin of the coordinate system at the center of the sphere. We call Δ the distortion, just for discussion purposes, and it is plotted in Fig. 2. As $\alpha\to 0$, Gaussian statistics are recovered, as expected. As α increases, there is a thumb-shaped region in the contour plot where the chain is flattened tangentially to the surface, with the most orientation occurring when $\beta \sim 0.6$–1.0. In addition, for small values of β and large values of α, we observe that the chain conformation is elongated away from the surface due to entropic repulsion. It is interesting that, for this geometry, there is a location where the tangential flattening is balanced by the entropic repulsion to result in a chain that has $\Delta = 0$, even though the Green's function for this condition is not spherically symmetric. For large α, the distortion of the wall case is recovered:

$$\Delta_W = -\frac{4\beta^2 erfc(\beta)}{erf(\beta)} + \frac{2\beta e^{-\beta^2}}{\sqrt{\pi} erf(\beta)} \tag{11}$$

Thus, there is a smooth transition between the wall case and the nanoparticle case. All of the deviations from Gaussian behavior occur when $\beta < {}^3/_2$. This predicts that the interphase is completely bounded 3 R_{g0} from the surface.

The segment density, c, for the polymer chain is calculated using [40]:

$$c(\vec{r},\vec{R},\vec{R'},N,a) = \frac{1}{G(\vec{R},\vec{R}',N,a)}\int_0^N dn\, G(\vec{R'},\vec{r},N-n,a)G(\vec{r},\vec{R},n,a) \tag{12}$$

It is the probability of finding a segment at a certain position $\vec{r}$, given that the polymer chain starts at $\vec{R}$ and ends at $\vec{R'}$. The next level of integration for this function is to inquire what the segment density is at any location if the chain end is allowed to range over all locations. This is known as the integrated segment density, H.

$$H(\vec{r},\vec{R},N,a) = \int d^3\vec{R'}\int_0^N dn\, G(\vec{R'},\vec{r},N-n,a)G(\vec{r},\vec{R},n,a) \tag{13}$$

The integral over $\vec{R'}$ is readily evaluated as the normalization constant for the Green's function, albeit for an altered chain length. Finally, if H is integrated over all possible origins of the chain, relative to the surface of the sphere, one arrives at the polymer segment density, F.

$$F(\vec{r},N,a) = \int H(\vec{r},\vec{R},N,a)d^3\vec{R} \tag{14}$$

The integration as written in equation (14) results in a non-uniform density of polymer segments surrounding the obstacle.

The polymer segment density around a sphere is thus given by:

$$F(r,N,a) = \frac{1}{N}\int_0^N \left[1-\frac{a}{r}erfc\left(\sqrt{\frac{N}{(N-n)}}x\right)\right]\left[1-\frac{a}{r}erfc\left(\sqrt{\frac{N}{n}}x\right)\right]dn \tag{15}$$

with

$$x = \frac{(r-a)}{2R_{go}} \tag{15a}$$

Following ref. [13], we derive the depletion width δ as a function of the radius of the sphere by solving the equation:

$$\frac{4\pi}{3}\left((a+\delta(N,a))^3-a^3\right) = 4\pi\int_a^\infty (1-F(r,N,a))r^2dr \tag{16}$$

The depletion width represents the thickness of a shell around the particle that balances the reduction in polymer segment density. We present the scaled depletion width $\delta/2R_{g0}$ in Fig. 3. The depletion width is zero as the nanoparticle radius tends to zero. It increases rapidly, achieving a very slight maximum of 0.353 in the curve at $\alpha = 1.14$ prior to leveling off at a value of 0.347. This implies that the depletion width ~ 0.7 R_{g0} for large α. This result is consistent with Fig. 7 from ref. [13], but comes to it from a different

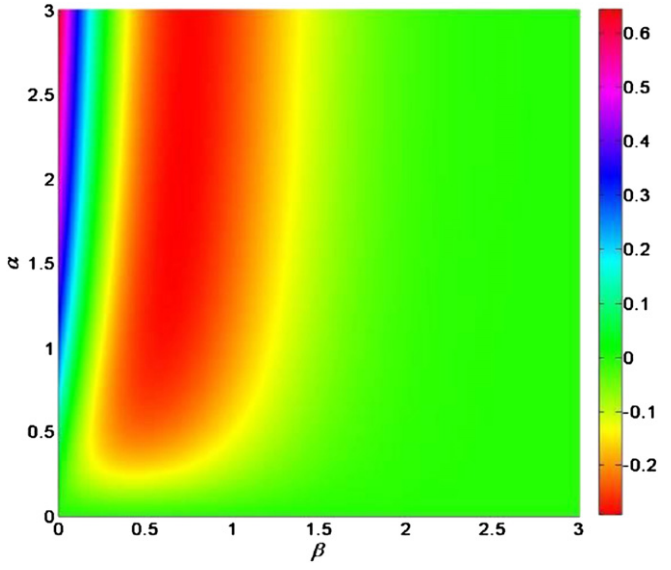

Fig. 2. Distortion in a polymer chain near a sphere. α is the scaled particle radius, and β is the scaled distance from the chain origin to the surface.

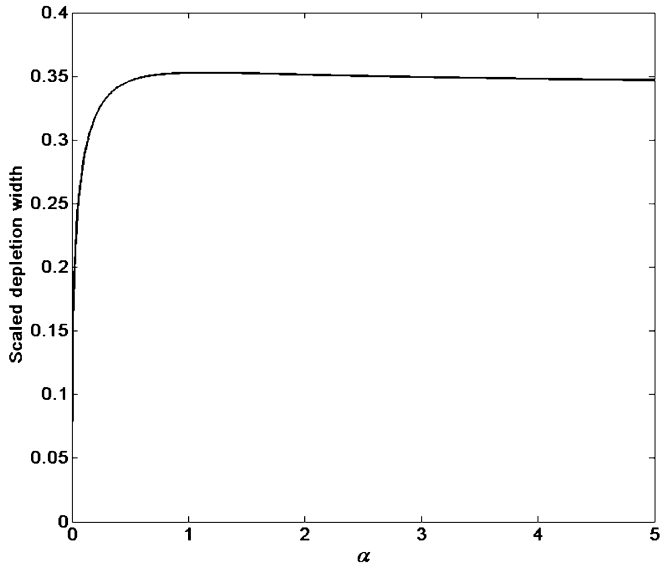

Fig. 3. Scaled depletion, $\delta/2R_{g0}$, width around a sphere.

functional form. As the radius of the sphere becomes large, equation (16) becomes:

$$F(y) = \frac{4\pi^2}{9N^3}\int_0^N \left(\sqrt{n}\sqrt{N-n}\right) erf\left(\sqrt{\frac{N}{n}}y\right) erf\left(\sqrt{\frac{N}{N-n}}y\right) dn \quad (17)$$

This integral is well-approximated by the usual expression $F(y) = \tanh^2(\pi^{1/2}\cdot y)$, where y is the distance from the wall scaled by $2R_{g0}$, and serves as another form for the solution to the problem of polymer segment density near a wall [13]. It is interesting to note the comparison between F and R_g. It is only when F deviates from unity that R_g deviates from unity. Thus, the distortions in the polymer conformation are occurring within the depletion region [41].

Alternatively, one can inquire what distribution of chain ends would result in a polymer segment density equal to unity for all positions. This is of concern because in a polymer melt, there is uniform segment density everywhere except within a distance that is atomistically close to the particle. This requires that chain ends be concentrated near the particle's surface. Mathematically, we inquire as to what chain end distribution function ψ solves the integral equation:

$$1 = \int H(\vec{r}, \vec{R}, N, a)\psi(\vec{R}, N, a)d^3\vec{R} \quad (18)$$

Generally, these integral equations are extremely difficult to solve. However, in this case, the solution is quite simple. We find that:

$$\psi(\vec{R}, N, a) = \frac{1}{F(\vec{R}, N, a)} = \frac{1}{F(b, N, a)} = \frac{1}{F(\alpha, \beta)} \quad (19)$$

is a solution to equation (18). This solution creates no depletion of polymer segment density at the surface of the sphere. This expression is equation (15) with a different variable for the radial distance. A depletion width accounting for the effects of screening due to polymer compressibility can be obtained by reducing the magnitude of F at small values of R.

3. Discussion

In this work, we describe the random walk probability distribution function perturbed by a spherical obstacle using the complete analytic Green's function. This approach has not been used previously by others working in the nanocomposite field. In addition, previous work using Green's functions has neglected to calculate the R_g of the polymer chain. It is this calculation that can model experimental scattering data. We have done this analysis for confined thin films and nanotubes [42], also.

Tuteja's characterization of linear polystyrene chains with polystyrene nanoparticle inclusions [28] provides interesting data to interpret in terms of the current work. That system should have minimal enthalpic contributions, and so should be well-approximated by our entropic theory. To do the comparison, we determine a value for α, given the measured radii of gyration of the polymer and the nanoparticle; see Table 1.

Next, we use the expression for surface-to-surface interparticle distance [43] to calculate an effective limiting value for the maximum distance of any chain origin from the surface of the nanoparticle.

$$\beta_{\lim} = \alpha\left(\left(\frac{\phi_{\max}}{\phi}\right)^{1/3} - 1\right) \quad (20)$$

We choose to use $\phi_{\max} = 2/\pi$ for random dense packing [44]. With this, we find that $\beta_{\lim}/\alpha = 3.00$, 1.34, and 0.85; for 1, 5, and 10 volume percent loadings, respectively. Notice in particular that $\beta_{\lim}/\alpha < 1$ at 10 v% loading. The average value, $\langle R_g/R_{g0}\rangle$, is then computed for this value of α, within the range $0 < \beta < \beta_{\lim}$, using the expression:

$$\left\langle \frac{R_g}{R_{g0}} \right\rangle = \frac{\int_0^{\beta_{\lim}} \frac{R_g(\alpha,\beta)}{F(\alpha,\beta)}(\alpha+\beta)^2 d\beta}{\int_0^{\beta_{\lim}} \frac{1}{F(\alpha,\beta)}(\alpha+\beta)^2 d\beta} \quad (21)$$

This is a volume average around the spherical inclusion. The kernel is the radius of gyration for a chain originating the scaled distance β from the surface, multiplied by the relative number of chain ends at that distance, and then multiplied by the differential volume of the shell. We have incorporated the chain end distribution function that the model predicts, $F(\alpha,\beta)$, following equations (18) and (19). The $(\alpha+\beta)^2$ term accounts for the volume of the shell around the sphere, akin to the $4\pi r^2$ term used in integrals performed in the spherical coordinate system. In this manner, $\langle R_g/R_{g0}\rangle$ can be predicted for all of Tuteja's experimental conditions. The results are shown in Fig. 4. Note that this is not a fit to the data. Rather, it is a comparison. There are no adjustable parameters in the model. At 1 v% and 5 v%, the agreement is within the error bars for most of the data points.

Table 1
Calculated values of α parameter.

Particle MW (kD)	Matrix MW (kD)	Particle Radius (nm)	Matrix R_g (nm)	α
25	65	2.0	5.7	0.18
52	65	2.7	5.7	0.24
135	65	3.6	5.7	0.32
25	235	2.0	11.4	0.088
52	235	2.7	11.4	0.12
135	235	3.6	11.4	0.16

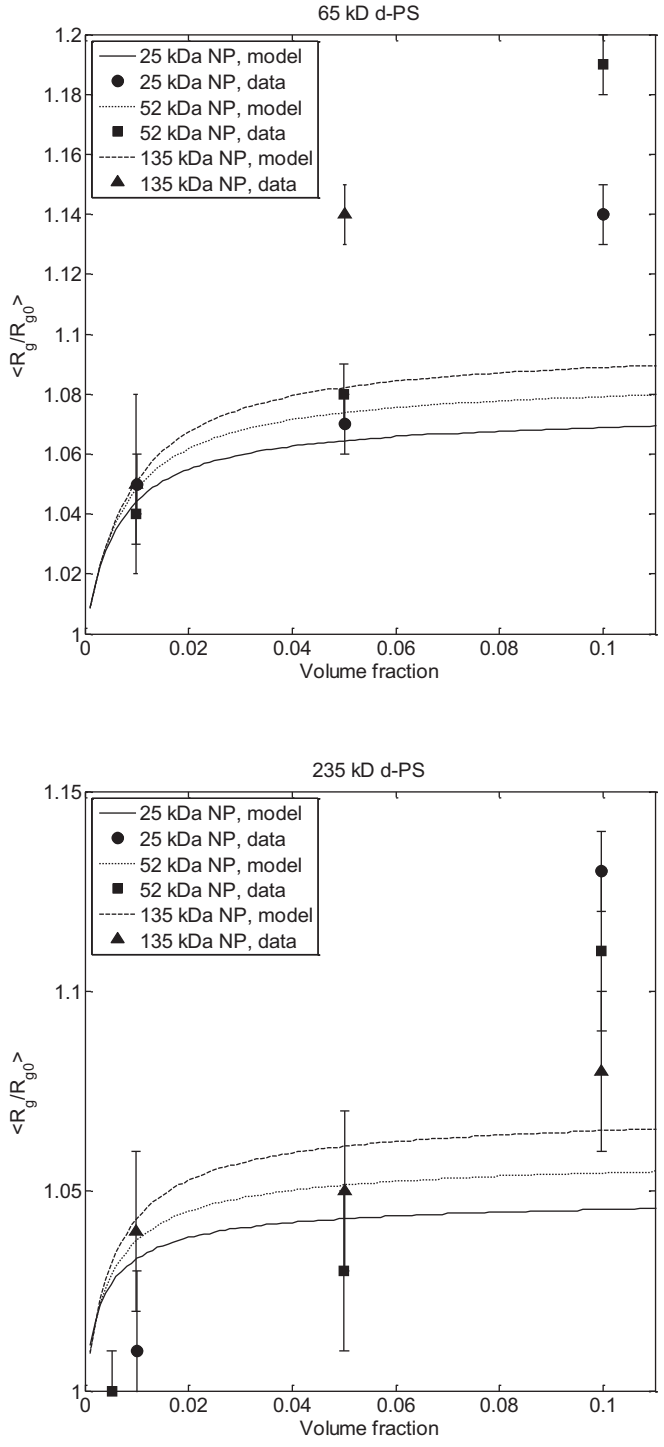

Fig. 4. Predicted values for the averaged, normalized radius of gyration as a function of loading, compared with the experimental data (ref. [33]).

At 10 v%, we clearly underestimate the measured values. While the data continues to increase, our theory flattens out. The source of this discrepancy lies in the fact that the theory is valid for a chain around a single particle. As the loading increases, the polymer chain is bounded by a space created by multiple particles, and the Green's function presented in equation (3) is no longer accurate; the situation is no longer a random walk around a single sphere. For reference, the interparticle distance is $<0.5\ R_{g0}$ at 10 v% for these samples. Thus, a single obstacle is no longer the appropriate model. This suggests that our model is not valid when $\beta_{\lim}/\alpha < 1$. The experimental results are showing that at high loadings, these polymer chains are not being confined to the interstice created by surrounding particles. Rather, they must be threading through several interstices, to be in accord with the experimental results. Another interpretation is that, at low loadings, the polymer chains expand when they encompass a single nanoparticle. At higher loadings, the chains encompass multiple particles, and the effects of expansion are simply additive.

Within the present model, we predict that $\langle R_g/R_{g0}\rangle$ could increase up to a maximum value of $(4/3)^{1/2} = 1.15$ if all chain ends were near the surface of the particle; this is close to the maximum expansion observed in the data. Thus it is possible to surmise that, at high volume loadings, there is more and more segregation of chain ends to the particle's surface. However, there is no evidence to support this, and it seems unlikely. Regardless, the fact that a single analytic theory can be applied to some of the situations in the data set is encouraging. It also suggests that, in this system, entropic effects can account for most of the observed increase in R_g at low loadings.

In our present analysis, we omitted the excluded volume parameter needed to model a self-avoiding walk. To include it in the Hamiltonian would result in a nonlinear term in equation (1), and preclude an analytic solution for this geometry. The exclusion of this term also implies that the model represents an incompressible polymer. This won't significantly affect the R_g and conformation analysis because, in a polymer melt, the scaling for $R_g \sim N^{1/2}$, which matches the result if excluded volume is omitted. However, it does have an effect on the segment density prediction. When there is a density fluctuation in a bulk material, the compressibility provides a force that smoothes out the variation. In the work done by Wu [45], they demonstrate that the inclusion of this term for the wall case results in a constant polymer segment density for distances greater than the screening length. The constant polymer segment density is achieved by a non-uniform chain end density. In our work, the use of the inverse of the polymer segment density as the chain end distribution function results in the chain end density being unbounded at the surface, but the prediction that the chain end density increases monotonically as the chain end approaches the surface is physically reasonable and observed in simulations [18]. Eliminating this term from equation (21), and thereby assuming a constant chain end distribution function, results in a decrease of a few percent in $\langle R_g/R_{g0}\rangle$, *i.e.*, values of ~ 1.07 become ~ 1.04. The shape of the curves are unchanged. Finally, our bulk segment density prediction is realistic for experimental polymer melts, and it grounds our results to the existing body of literature regarding depletion width in colloids [13,41].

It is difficult to compare our theory to others, since different properties are presented. We can compare our results with that of Starr [26]. Studying that work, we deduce that their calculation was performed with a nanoparticle and polymer chain size such that the value of $\alpha \sim 1$. For the case of non-attractive interactions, they calculated that R_g increased by a factor of ~ 1.10 as the center-of-mass of the polymer chain approached the surface of the sphere. In our calculations, as the chain end approaches the surface of the sphere, R_g increases by factor of 1.14 when $\alpha \sim 1$, which is within Starr's error bars. The minimum in R_g that we calculate for the wall case at $\beta \sim 1$ is barely visible when $\alpha \sim 1$, which also agrees with their calculations. We can also compare our results to those presented in Fig. 1 of Frischknecht [27]. Below 5 v%, there is good agreement between the two methods. Unfortunately, we cannot compare to Termonia's [18] or Vacatello's [20] calculations because their work was done at high volume loadings, where our theory is not applicable. All theories predict a flattening of the chain against the particle.

Our analysis does not contradict other experimental work, either. In the case of Sen's work [29], the aggregation that they observe effectively increases the value of α that goes into our model.

Performing a volume average in that case results in very little increase in R_g because most chains are not near the surface of a filler particle. The work by Jones on thin films [30] can be explained by the observation detailed in the Appendix, equation (A.5), which shows that the R_{ee} in the plane of the film would retain its Gaussian value, regardless of the position of the chain end from the wall. For Nakatani's data [32], meaningful comparisons are not possible because their data is acquired at very high volume loadings.

To account explicitly for enthalpic interactions in this model would be difficult. However, one could posit that an attractive enthalpic interaction would create multiple interactions between a chain and the particle. This could then be modeled with Green's functions as a statistical distribution of loops, trains, and tails for a chain near the surface. Still, the simplest method to model enthalpy is to consider the polymer-at-a-wall situation, and provide a nonzero monomer density at the wall by making the source strength greater than the sink strength. This will be investigated in more detail in the future. We predict that this can counter the entropic repulsion, making the polymer conformation more tangential to the surface, and muting the increase in R_g. Another consequence of enthalpic interactions could be observed in polydisperse polymer melts. A polymer chain with higher molecular weight may be more likely to be adsorbed to a particle than a shorter chain. This could result in a segregation of longer chains to the surface region, which could affect the melt viscosity.

Finally, it is worth noting what this theory predicts about the entanglement density of polymeric nanocomposites. The discussion on this subject relates the volume pervaded by the polymer chain to the entanglement density; the larger the spatial extent of the chain, the greater the entanglement density [46,47]. Since our model predicts that R_g increases for chains near spheres, we would posit that the entanglement density is increased in the region close to the spheres. If chain ends segregated to the sphere's surface, it would reinforce this supposition. Also, we see from Fig. 1 that, in some cases, there is a reduction in R_g near the sphere, and this would correspond to a reduction in the entanglement density. The polymer would form a shell around the sphere of thickness $\sim 2\,R_{g0}$, within which the entanglement density would be higher than the bulk, while at the surface of the shell, the entanglement density is slightly less than the bulk value. This may imply the existence of a boundary layer around each inclusion, which could affect viscosity in the melt.

4. Conclusions

We have described the size and shape of polymer chains in the vicinity of a sphere, and demonstrated the smooth transition between a flat wall and a sphere. This entropic theory provides an analytical extension to the polymer-at-a-wall theories that has not been presented in the literature to date. We have shown that the radius of gyration of the polymer chain contracts as the chain end approaches the obstacle, and then expands upon further approach. The shape of the polymer chain is flattened tangentially to the surface at intermediate distances, and then extends radially due to entropic repulsion at close distances. Direct comparison to data shows that the model can account for the observed increases in R_g of polymer chains in low-loaded nanocomposites as measured by neutron scattering. As such, the theory is a useful model for the structure of the interphase in polymeric nanocomposites.

Appendix A. Random walk near a wall

This problem has been considered previously in the literature [13,37,45,48]. Here we briefly state the results relevant to this work. The Green's function for a random walk near an impenetrable wall is:

$$G(r,z,N,b) = \exp\left(-\frac{r^2}{4R_{g0}^2}\right)\left\{\exp\left(-\frac{z^2}{4R_{g0}^2}\right) - \exp\left(-\frac{(z+2b)^2}{4R_{g0}^2}\right)\right\} \tag{A.1}$$

The z-direction is perpendicular to the wall, and the r-direction is parallel to it; cylindrical symmetry is used. The origin of the chain is at the origin of the coordinate system. Thus, the wall is located at $z=-b$. The relevant integral averages are:

$$G_{W,0} = \int_{-b}^{\infty}\int_{0}^{2\pi}\int_{0}^{\infty} G(r,z,N,b)\,r\,dr\,d\theta\,dz = \left(\sqrt{4\pi R_{g0}^2}\right)^3 erf(\beta) \tag{A.2}$$

$$G_{W,r} = \int_{-b}^{\infty}\int_{0}^{2\pi}\int_{0}^{\infty} r^2 G(r,z,N,b)\,r\,dr\,d\theta\,dz = \left(\sqrt{4\pi R_{g0}^2}\right)^3 4R_{g0}^2 erf(\beta) \tag{A.3}$$

$$G_{W,z} = \int_{-b}^{\infty}\int_{0}^{2\pi}\int_{0}^{\infty} z^2 G(r,z,N,b)\,r\,dr\,d\theta\,dz = \left(\sqrt{4\pi R_{g0}^2}\right)^3 2R_{g0}^2\left(erf(\beta) - 4\beta^2 erfc(\beta) + \frac{2\beta}{\sqrt{\pi}}e^{-\beta^2}\right) \tag{A.4}$$

In these expression, $\beta = b/(2R_{g0})$, as in the main text. From this, we derive:

$$\left\langle r^2\right\rangle = \left\langle x^2\right\rangle + \left\langle y^2\right\rangle = 4R_{g0}^2 \tag{A.5}$$

$$\left\langle z^2\right\rangle = 2R_{g0}^2\left(1 - 4\beta^2\frac{erfc(\beta)}{erf(\beta)} + \frac{2\beta}{\sqrt{\pi}}\frac{e^{-\beta^2}}{erf(\beta)}\right) \tag{A.6}$$

The mean-squared end-to-end distance normalized to that of a Gaussian chain is then:

$$\frac{R_{ee,W}^2}{R_{ee0}^2} = \frac{\left\langle r^2\right\rangle + \left\langle z^2\right\rangle}{6R_{g0}^2} = \frac{1}{3}\left(3 - 4\beta^2\frac{erfc(\beta)}{erf(\beta)} + \frac{2\beta}{\sqrt{\pi}}\frac{e^{-\beta^2}}{erf(\beta)}\right) \tag{A.7}$$

The radius of gyration is calculated:

$$R_g^2 = \frac{1}{2N^2}\sum_{n=1}^{N}\sum_{m=1}^{N}\left\langle (R_n - R_m)^2\right\rangle \tag{A.8}$$

$$\left\langle (R_n - R_m)^2\right\rangle = \sigma'^2\left[3 + 4\beta'^2 - \frac{4\beta'^2}{erf(\beta')} + \frac{2\beta e^{-\beta'^2}}{\sqrt{\pi}erf(\beta')}\right] \tag{A.9}$$

$$\sigma'^2 = \frac{|n-m|l^2}{3} \tag{A.10}$$

Where $\beta' = b/(2^{1/2}\sigma')$. The elements of the conformation tensor are:

$$C_{zz} = 1 - \frac{4\beta^2 erfc(\beta)}{erf(\beta)} + \frac{2\beta e^{-\beta^2}}{\sqrt{\pi}erf(\beta)} \tag{A.11}$$

$$C_{xx} = C_{yy} = C_{rr}/2 = 1 \tag{A.12}$$

When combined, they yield equation (11) of the main text. Furthermore, when equation (A.1) is used as the input to equations (2)–(14) of the main text, equation (17) results.

Appendix B. Derivation of equation (6)

To derive equation (6) from equation (5), one first performs the integration over $\overrightarrow{R}'$ in equation (5), resulting in the normalization integral equation (4). This is shown in equation (B.1), which explicitly includes the limits of the integral, from the surface of the particle to infinity. In this expression, the location of the chain end from the surface of the sphere, defined as b in the text, becomes the variable of integration, and is renamed r.

$$\Omega = \int\int G(\overrightarrow{R},\overrightarrow{R}',N,a)\,d^3\overrightarrow{R}\,d^3\overrightarrow{R}' = \int G_0(R,N,a)\,d^3\overrightarrow{R} = 4\pi\int_a^\infty\left(1-\frac{a}{r}erfc\left(\frac{r-a}{2R_{g0}}\right)\right)r^2dr \tag{B.1}$$

For the Gaussian case,

$$\Omega_0 = \int d^3\overrightarrow{R} = 4\pi\int_0^\infty r^2dr = 4\pi\int_0^a r^2dr + 4\pi\int_a^\infty r^2dr \tag{B.2}$$

Constructing the difference between the two gives:

$$\Omega_0-\Omega = 4\pi\int_0^a r^2dr + 4\pi\int_a^\infty r^2dr - 4\pi\int_a^\infty r^2dr + 4\pi\int_a^\infty\left(\frac{a}{r}erfc\left(\frac{r-a}{2R_{g0}}\right)\right)r^2dr \tag{B.3}$$

The middle two integrals cancel identically, while the remaining integrals simplify to equation (6) of the main text [49].

Appendix C. Calculating R_g^2

Equation (8) is the strict definition presented by Doi and Edwards [40]. It expresses R_g^2 in terms of the $\langle R_{ee}^2\rangle$ between all pairs of monomers in the chain. Equation (7) provides $\langle R_{ee}^2\rangle$ for any value of N, the number of monomers. Recall equation (8):

$$R_g^2(\overrightarrow{R},N,a) = \frac{1}{2N^2}\sum_{n=1}^{N}\sum_{m=1}^{N}\left\langle(R_n-R_m)^2\right\rangle \tag{C.1}$$

Next, realize that in equation (7), $\langle R_{ee}^2\rangle$ is a function of the distance between the monomers, with the location of one monomer as a separate parameter R, or equivalently, b. Now, in equation (C.1), the term in brackets on the right-hand-side is the statistically averaged end-to-end distance squared between two monomers of a chain that is $(n-m)$ units long, as opposed to N units long for the whole chain. Equation (7) can also be used to calculate $\langle R_{ee}^2(b,(n-m),a)\rangle$. Thus, the terms in the summation can be individually calculated. Since these terms only depend on $k=(n-m)$, the double summation can be reduced to a single summation. In the double summation, there are no terms with N steps, 1 term with N-1 steps, 2 terms with N-2 steps, etc., until one reaches N-2 terms with two steps, and N-1 terms with one step. So the double sum is commuted to a single sum. In this manner, equation (C.1) is transformed to:

$$R_g^2(b,N,a) = \frac{1}{N^2}\sum_{k=1}^{N-1}(N-k)\left\langle R_{ee}(\alpha',\beta')\right\rangle \tag{C.2}$$

Where $\alpha' = a/(\sqrt{2}\sigma)$, $\beta' = b/(\sqrt{2}\sigma)$, and $\sigma^2 = kl^2/3$. In execution, $\langle R_{ee}^2\rangle$ was calculated for the entire range of α' and β' of interest to the problem, then the summation was computed.

References

[1] Paul DR, Robeson LM. Polymer 2008;49:3187–204.
[2] Vaia RA, Maguire JF. Chem Mater 2007;19:2736–51.
[3] Schaefer DW, Justice RS. Macromolecules 2007;49:8501–17.
[4] Forrest JA, Dalnoki-Veress K. Adv Colloid Interface Sci 2001;94:167–96.
[5] Alcoutlabi M, McKenna GB. J Phys Condens Matter 2005;17:R461–524.
[6] Bogoslovov RB, Roland CM, Ellis AR, Randall AM, Robertson CG. Macromolecules 2008;41:1289–96.
[7] Johnsen BB, Kinloch AJ, Mohammed RD, Taylor AC, Sprenger S. Polymer 2007;48:530–41.
[8] Schadler LS, Brinson LC, Sawyer WG. JOM 2007;59:53–60.
[9] Ash BJ, Siegel RW, Schadler LS. Macromolecules 2004;37:1358–69.
[10] Ramanathan T, Abdala AA, Stankovich S, Dikin DA, Herrera-Alonso M, Piner RD, et al. Nat Nanotechnology 2008;3:327–31.
[11] Rowland HD, King WP, Pethica JB, Cross GLW. Science 2008;322:720–4.
[12] Napper DH. Polymeric stabilization of colloidal dispersions. London: Academic Press; 1983.
[13] Fleer GJ, Skvortsov AM, Tuinier R. Macromolecules 2003;36:7857–72.
[14] Eisenriegler E. J Chem Phys 1983;79:1052–64.
[15] Russel WB, Saville DA, Schowalter WR. Colloidal dispersions. Cambridge: Cambridge University Press; 1989.
[16] Fleer GJ, Stuart MAC, Scheutjens JMHM, Cosgrove T, Vincent B. Polymers at interfaces. London: Chapman & Hall; 1993.
[17] Ozmusul MS, Picu CR, Sternstein SS, Kumar SK. Macromolecules 2005;38:4495–500.
[18] Termonia Y. Polymer 2009;50:1062–6.
[19] Vacatello M. Macromolecules 2001;34:1946–52.
[20] Vacatello M. Macromolecules 2002;35:8191–3.
[21] Vacatello M. Macromol Theory Simul 2006;15:303–10.
[22] Allegra G, Raos G, Vacatello M. Prog Polym Sci 2008;33:683–731.
[23] Sharaf MA, Mark JE. Polymer 2004;45:3943–52.
[24] Mark JE, Abou-Hussein R, Sen TZ, Kloczkowski A. Polymer 2005;46:8894–904.
[25] Yuan W, Kloczkowski A, Mark JE, Sharaf MA. J Polym Sci Part B Polym Phys 1996;34:1647.
[26] Starr FW, Schroder TB, Glotzer SC. Macromolecules 2002;35:4481–92.
[27] Frischknecht AL, McGarrity ES, Mackay ME. J Chem Phys 2010;132. 204901-1-204901-6.
[28] Tuteja A, Duxbury PM, Mackay ME. Phys Rev Lett 2008;100. 077801-1-077801-4.
[29] Sen S, Xie Y, Kumar SK, Yang H, Bansal A, Ho DL, et al. Phys Rev Lett 2007;98. 128302-11-128302-4.
[30] Jones RJ, Kumar SK, Ho DL, Briber RM, Russell TP. Nature 1999;400:146–9.
[31] Jones RJ, Kumar SK, Ho DL, Briber RM, Russell TP. Macromolecules 2001;34:559–67.
[32] Nakatani AI, Chen W, Schmidt RG, Gordon GV, Han CC. Polymer 2001;42:3713–22.
[33] Nakatani AI, Chen W, Schmidt RG, Gordon GV, Han CC. Int J Thermoplastics 2002;23:199–209.
[34] Mavrantzas VG, Theodorou DN. Macromolecules 1998;31:6310–32.
[35] Carslaw HS, Jaeger JC. Conduction of heat in solids. New York: Oxford; 1959.
[36] Doi MJ. Phys A Math Gen 1975;8:417–26.
[37] Eisenriegler E, Hanke A, Dietrich S. Phys Rev E 1996;54:1134–52.
[38] Aarts DGAL, Tuinier R, Lekkerkerker HNW. J Phys Condens Matter 2002;14:7551–61.
[39] Louis AA, Bolhuis PG, Meijer EJ. Chem Phys 2002;116:10547–56.
[40] Doi M, Edwards SF. The theory of polymer dynamics. New York: Oxford; 1986.
[41] Doxastakis M, Chen Y-L, Guzman O, de Pablo JJ. J Chem Phys 2004;120:9335–42.
[42] J.S. Meth, S.R. Lustig. Submitted for publication.
[43] Wu S. Polymer 1985;26:1855–63.
[44] German RM. Particle packing characteristics. New Jersey: Metal Powder Industries Federation; 1989.
[45] Wu DT, Fredrickson GH, Carton J-P, Ajdari A, Liebler LJ. Polym Sci B Polym Phys 1995;33:2373–89.
[46] Brown HR, Russell TP. Macromolecules 1996;29:798–800.
[47] Si L, Massa MV, Dalnoki-Veress K, Brown HR, Jones RAL. Phys Rev Lett 2005;94:127801.
[48] Brazhnik PK, Freed KF, Tang HJ. Chem Phys 1994;101:9143–54.
[49] Gradshteyn IS, Ryzhik IM. Table of integrals, series, and products. San Diego: Academic; 1980. Formula 6.281.1.